Wavelet Thresholding Technique for sEMG Denoising by Baseline Estimation

Abstract. The surface Electromyography (sEMG) signal is affected by different sources of noises: current technology is considerably robust to the interferences of the power line or cable motion artifacts, but still there are many limitations in denoising the baseline. In this paper we introduce a new technique, named Baseline Adaptive Denoising Algorithm (BADA), for denoising the sEMG signal by wavelet thresholding procedure. In particular, the thresholds are estimated using the same baseline signal with fixed and adaptive techniques. Eventually, we verify that the proposed adaptive method performs better than the standard Donoho technique and different variations, in term of noise cancellation and distortion of the signal, quantified by a new suggested indicator of the denoising quality.

Keywords: Wavelet Denoising, Surface Electromyography.

Introduction

Surface Electromyography (sEMG) provides a safe, easy and non-invasive method to qualitatively and quantitatively analyze the activity of the muscles (Cram et al. 1998; Merletti and Parker 2004): unlike needle EMG, where the procedure is performed invasively by inserting needles through the skin into the muscle, the sEMG examination evaluates muscle function by recording activity from the surface above the muscle on the skin. Currently, sEMG is widely applied for the assessment in sport (Knudson and Blackwell 2000; Hernandez et al. 2010), rehabilitation (Lange et al. 1996; Kibler et al. 2008), ergonomic design (Gazzoni 2010; Troiano et al. 2008), and medical robotics (Zecca et al. 2002).

However, the sEMG is affected by various sources of noises, including the power line interference, the noise generated by the cable motion, the baseline and the movement artifact noise. In particular, the baseline is the combination of the two noise sources originated in the electronics of the amplification system (thermal noise) and at the skin-electrode interface (electrochemical noise), respectively (De Luca et al. 2010; Huigen et al. 2002).

While the power line interference and the cable motion artifact can be removed using standard filtering procedures (Cram et al. 1998; Basmajian and De Luca 1985), the baseline and the movement artifact have spectra

that include also the low frequency spectrum of the EMG signal: a standard filtering risks to alter important information of the signal. The solution is to filter the maximum quantity of noise while keeping as much of the effective signal frequency spectrum as possible.

Wavelet denoising algorithms have been received extensive consideration in the processing of white Gaussian noise in biological signals, especially for the Electrocardiogram (Rosas-Orea et al. 2005; Blancovelasco et al. 2008). Most wavelet based denoising literatures suggest the use of the Donoho's method (Donoho and Johnstone 1994; Donoho 1995), that estimates the thresholds by maximizing a risk function in terms of quadratic loss at the sample points. Though, considering that the baseline is not a white Gaussian noise, this method has limitations in the denoising of EMG signal, because it removes also significant part of signal with a consequent loss of geometrical characteristics of the signal. Different studies (Phinyomark et al. 2009; Jiang and Kuo 2007) have proposed to change the thresholds using different statistical techniques, with some improvements in the denoising, but still the results have not been completely confirmed and the hypothesis is white Gaussian noise.

This paper presents the development of a new method to denoise the sEMG signal using the baseline to estimate the thresholds of the Wavelet denoising algorithm, named Baseline Adaptive Denoising Algorithm (BADA). This is an extension of preliminary results shown in (Bartolomeo et al. 2011). In this work we apply the algorithm for a more complex exercise, the peg-board, used in the training of young surgeons to improve the manual skill (Derossis et al. 1998).

The organization of the paper is as follows: at first we introduce the theory of the Wavelet denoising algorithm and we list the different thresholds used to benchmark the proposed algorithm, referred in (Donoho 1995; Donoho 1993; Guoxiang and Ruizhen 2001; Zhong and Cherkassky 2000). After, we describe our experimental setup and explain the evaluation method to compare the different methods and the proposed algorithm. Finally, comparing the results with other algorithms, we prove that our method achieves better noise rejection during the noisy interval and higher likelihood with the original signal during the exercise interval.

Wavelet denoising algorithm

A. Overview

Given a general model of a noisy signal $s(n)=f(n)+e(n)$, the objective of

the Wavelet denoising algorithm is to discard the noise part *e(n)* of a signal *s(n)* and to recover *f(n)*. The term *e(n)* is usually considered a white Gaussian noise.

The procedure of wavelet denoising is composed of three steps.

1. Decomposition. The original signal is decomposed by using the Stationary discrete Wavelet Transform (SWT). The SWT is preferred to the simple Discrete Wavelet Transform (DWT) because it has the property to be invariant to translations, eliminating visual artifacts like Gibbs phenomena in the neighborhood of discontinuities (Coifman and Donoho 1995). This first step requires the choice of the mother wavelet and the level of decomposition *J*. The details cD_j and approximation cA_j coefficients for each level *j* are obtained by the multi-resolution analysis (Shensa 1992).
2. Thresholding. For each level of decomposition the detail coefficients are compared with a level of threshold, then the signal is suppressed or transformed if it is smaller than the threshold. This second step requires the choice of the thresholds and the transformation function for the different levels of decomposition.
3. Reconstruction. The denoised signal is reconstructed by applying the Inverse Stationary Wavelet Transform (ISWT) to the approximation coefficient at level *J* and modified detail coefficients from level 1 to *J*.

Figure 1 Flow chart of the Wavelet denoising algorithm.

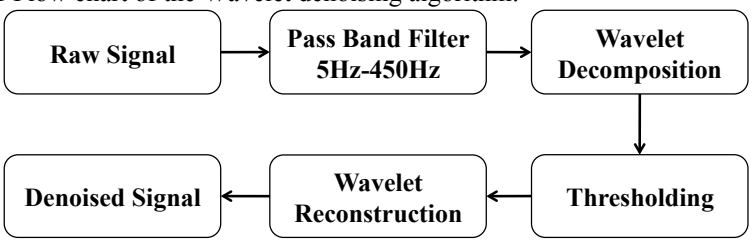

Figure 2 Wavelet function Daubechies db2

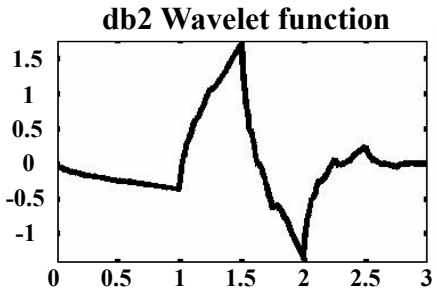

The summarized denoising algorithm is shown in Figure 1.

For this work we have considered the Daubechies db2 mother wavelet, shown in Figure 2, and the forth decomposition level, as they have been proved, in case of myoelectric signals, to have the lowest mean square error (Phinyomark et al. 2009; Bartolomeo et al. 2011). This paper focuses on the determination of the appropriate threshold.

B. Thresholding

The selection of the threshold is of paramount importance in the Wavelet denoising algorithm. Usually the universal threshold (*UNI*) proposed by Donoho and Johnstone (Donoho and Johnstone 1994) is used as comparison to evaluate new techniques of denoising, due to its conservative nature (Johnstone and Silverman 1997). Universal threshold estimation method uses a fixed value,

$$THR_{UNI} = \sigma\sqrt{2\log(N)} \tag{1}$$

where N is the length of the samples of the time-domain signal and σ is estimated as the median of the absolute value of the detailed coefficients at the decomposition level j, divided by 0.6745, a normalization factor used to rescale the numerator to make the estimate unbiased for the normal distribution (Donoho and Johnstone 1994).

In this work we have compared the proposed denoising technique also with other thresholds using different criteria such as:

1. SURE (Stain's Unbiased Risk Estimate), in which the threshold is calculated minimizing the Stein Unbiased Estimate of Risk (Donoho and Johnstone 1995; Stein 1981).
2. Modification of the universal threshold for soft thresholding (Donoho 1995), in which the universal threshold is scaled by the length of the samples in time domain. In (Phinyomark et al. 2009) this modification is defined as *Length Modified Universal Method (LMU)*:

$$THR_{LMU} = \sigma\sqrt{\frac{2\log(N)}{N}} \tag{2}$$

3. *Scale Modified Universal Method (SMU)* (Donoho 1993), in which the universal threshold is modified as:

$$THR_{SMU} = \sigma 2^{\frac{j-J}{2}}\sqrt{2\log(N)} \tag{3}$$

where the J is the total number of decomposition levels and j is the current scale level.

4. *Scale Length Modified Universal Method (SLMU)* (Donoho 1993), where *LMU* and *SMU* are combined as:

$$THR_{SLMU} = \sigma 2^{\frac{j-J}{2}} \sqrt{\frac{2log(N)}{N}} \tag{4}$$

5. *Log Scale Modified Universal Method (LSMU)*, proposed by (Guoxiang and Ruizhen 2001)

$$THR_{LSMU} = \sigma \frac{\sqrt{2log(N)}}{log(j+1)} \tag{5}$$

6. *Global Scale Modified Universal Method (GSMU)*, proposed by (Zhong and Cherkassky 2000). This method in (Phinyomark et al. 2009) has shown the better denoising performance for six motions of hand, compared with the other in the list:

$$THR_{GSMU} = \sigma 2^{-\frac{J}{2}} \sqrt{2log(N)} \tag{6}$$

The way to apply the threshold is standard: for each level of decomposition the detail coefficients are compared with the threshold, and then the signal is suppressed or transformed if it is smaller than the threshold. Common ways to modify the signal after the level comparisons are the Hard and Soft Thresholding. In the Hard Thresholding (HT) the detail coefficient is completely suppressed if its absolute value is smaller than the threshold:

$$cD_j = \begin{cases} cD_j & if \left|cD_j\right| \geq THR_j \\ 0 & otherwise \end{cases} \tag{7}$$

where the THR_j is the selected threshold at level j.

Differently, in the Soft Thresholding (ST) the signal is linearly shrunk as follows:

$$cD_j = \begin{cases} cD_j - THR_j & \text{if } cD_j \geq THR_j \\ 0 & \text{if } \left|cD_j\right| < THR_j \\ cD_j + THR_j & \text{if } cD_j \leq -THR_j \end{cases} \tag{8}$$

The ST modifies the original signal, introducing a bias, but on the other hand it reduces the non-linearities, which instead are introduced by the HT. The choice of one or another really depends on the applications and expected results. For the general aim of this study, we have decided to compare the various thresholds with both of the modifications. The proposed threshold is calculated by using the adaptive algorithm presented

later in the paragraph Baseline Adaptive Denoising Algorithm (BADA).

Experimental setup

A. Hardware

The sEMG signals have been recorded on the Extensor Carpi Ulnaris (R-ECU and L-ECU for the right and left arm), the Flexor Carpi Radialis (R-FCR and L-FCR), the Biceps Brachii (R-BB and L-BB), the Triceps Brachii (R-TB and L-TB), the Left Trapezius (LT), the Right Trapezius (RT), in addition to two electrodes on the left Corrugator Supercilii (CS) and Zygomaticus Major (ZM) for the facial EMG analysis. The location of the sensors is shown in Figure 3 .We used surface DE-2.1 sensors (Delsys Inc.) and the signal were amplified by a BagnoliTM 16-channel system (Delsys Inc.) with a Gain K=100. The skin was cleaned by mildly scrubbing it with 70% isopropyl alcohol. The sensors were attached to the skin with a double-sided adhesive interface. The sEMG sensor was located in the midline of the muscle belly between the nearest innervation zone and the myotendinous (De Luca 1997). A Dermatrodes HE-R (American Imex) electrode (5.08 cm dia.) was placed on the iliac crest to provide a reference. Sampling rate was set at 1000 samples per second using a 16-bit A/D converter board (National Instruments, USA, PCI-6034E). The acquisition software has been developed in C++ and data have been processed using MATLAB 7.7 (R2008b).

Figure 3 sEMG sensor location: a. R-FCR, b. R-BB, c. R-ECU, d. R-TB, e. L-FCR, f. L-BB, g. L-ECU, h. L-TB, i. LT, j. RT, k. CS, l. ZM.

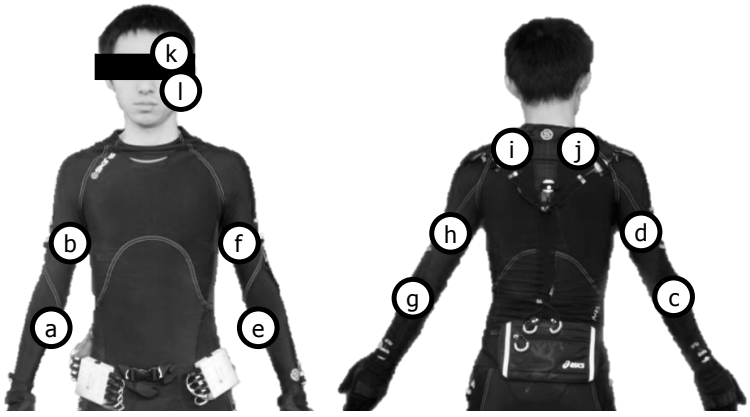

B. Task and protocol

Fifteen subjects participated to this experiment, with an average age of 24 years old. The measurements have been taken during 20 trials of a peg-board practice, for each subject, in which they used laparoscopes to move sequentially a set of rubber O rings positioned inside pegs. This laparoscopic task is widely recognized to train surgeons in manual skill (Derossis et al. 1998). The peg-board practice is a technique in which the trainee is using forearms, arms, and shoulders; additionally it is an exercise that we can easily perform in our laboratory because we have a dry box with all the equipment for the laparoscopic training (Lin et al. 2010).

After a brief explanation session, all the subjects signed an informed consent. Before the practice, each trainee was prepared following this procedure:

1. *Explanation session:* the experimenter explained the details of the practice, showing the training box and how to use the laparoscopes. In this way the subject could ask some questions also during the hardware setup.
2. *EMG sensors positioning:* after placing the reference on the iliac crest, each sensor was placed on the relative muscle; by monitoring the real time data on the PC, the best position was selected; finally, an elastic band, in addition to the double-faced adhesive interface, was placed around the sensor.
3. *MVC recording:* Maximum Voluntary Contraction (MVC) was recorded for each muscle under measurement, in order to normalize the signals during the post-processing: the procedure has been done with a muscle positioned within its midrange length, against manual resistance. Following the indications in (Cram et al. 1998) the central 2 seconds of a 6 to 8 seconds MVC period have been recorded and averaged over three trials.
4. *Baseline Recording:* the trainee was asked to stay 10s completely relaxed standing in front of the training box. A visual check from the experimenter was done during this phase, especially for the facial expression.

After the preparation the subject was asked to perform a not recorded trial, during which the system was tested.

Evaluation method

By using the information coming from the *Baseline Recording*, an only-

noise portion of the signal is separated from a task portion. Indicating $n_o(n)$ the noise portion of the signal, and $n_d(n)$ the noise portion after the denoising, they are compared with a Noise Ratio (NR):

$$NR = \frac{RMS\left(n_d(T)\right)}{RMS\left(n_o(T)\right)},\ T \in \text{ Baseline Portion} \tag{9}$$

where the RMS indicates the root mean square and T is the interval of the baseline portion. With this approach it is possible to have a number related only to the baseline segment of the signal. The smaller this value, the higher the quality of the noise rejection will be.

Additionally, denoting $t_o(n)$ the waveform of the task portion of the original signal and $t_d(n)$ the one after the denoising procedure, they are compared by using an error function that measures the misfit, point by point, of the two functions, given by the sum of the squares of the differences, divide by the RMS of $t_o(n)$:

$$E_t = \frac{1}{2}\sum_{j=1}^{N}\left(\frac{t_o(j) - t_d(j)}{RMS\left(t_o\right)}\right)^2 \tag{10}$$

where N is the number of the samples in the exercise portion. To facilitate the analysis, we consider the RMS value of E_t:

$$ER = \sqrt{\frac{2E_t}{N}} \tag{11}$$

where N is the number of samples in the exercise portion and it is used to normalize the error to compare different sizes of signal in equal way.

Figure 4 The ER is calculated on the portions $t_o(n)$ of the rectified signal over a threshold defined by the RMS of the entire signal.

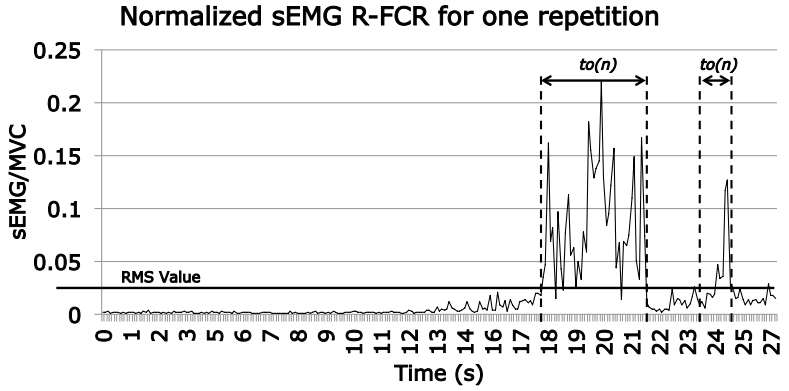

The smaller the *ER* is, the smaller the distortion due to the denoising algorithm will be. The $t_o(n)$ is defined by the portions of signal over a threshold defined by the total RMS value, as shown in Figure 4.

We propose the combination of these two parameters to give an estimation of the denoising quality and to compare different methods.

$$DQ_{\%} = 1 - \left(\alpha_{NR} NR + \alpha_{ER} ER\right) \qquad \alpha_{NR} + \alpha_{ER} = 1 \tag{12}$$

where $DQ_{\%}$ indicates the quality of the denoising in percentage, α_{NR} is the weight of the noise ratio and α_{ER} is the weight of the distortion. For our evaluation we have chosen α_{NR}=0.7 and α_{ER}=0.3, giving more importance to the noise reduction than distortion. In our results we are going to show the *DQ%* for different values of the weights.

Baseline Adaptive Denoising Algorithm (BADA)

The Donoho method and its derivatives have been considered suitable for the denoising of sEMG, because the baseline has been approximated as a white Gaussian noise, distributed equally on the entire spectra of the signal. In case of the sEMG Baseline, however, this approach is not valid, because the spectrum of the Baseline is not a white Gaussian noise (Figure 5).

Figure 5 Spectrum of the Baseline. It is not a white Gaussian noise.

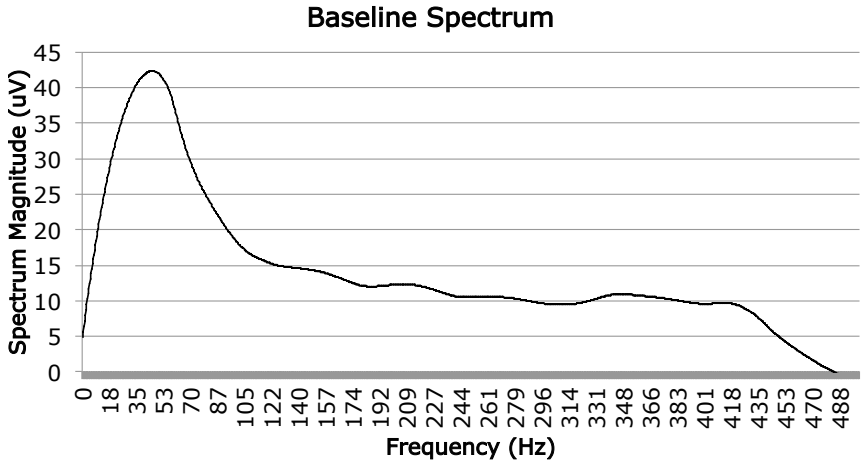

Our approach is to clean the signal from a baseline that is not a white Gaussian noise. Based on this consideration, the proposed algorithm derives the thresholds in the following way:

Baseline Adaptive Denoising Algorithm (BADA): the thresholds are calculated in order to reduce, for each level of decomposition, the noise level down to 1%. As shown in Figure 6, the algorithm keeps in memory the original RMS value of the detail coefficient, which is also the first Threshold applied to it. After, the RMS of the modified detailed is calculated, and, if the new RMS is bigger than 1% of the original one, the threshold is updated by increasing of 10% respect to the previous value.

Figure 6 BADA algorithm. The thresholds are chosen in order to reduce the noise, for each level of decomposition, down to 1%.

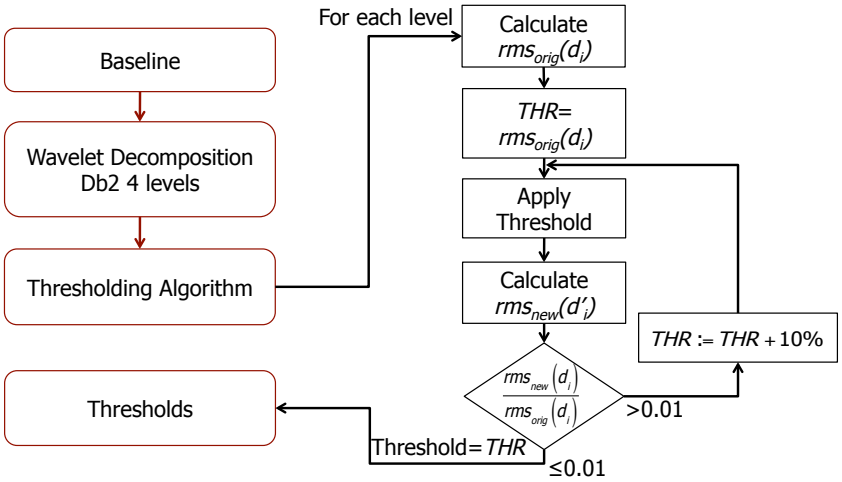

Results and discussion

The averaged results of the $DQ_{\%}$, together with the standard deviations, for the fifteen subjects for all the muscles are summarized in Tables 1-6. Each table is divided in two parts: the first presents α_{NR}=0.7 and α_{ER}=0.3, the noise reduction is considered more important that the distortion of the signal; the second has α_{NR}=0.3 and α_{ER}=0.7, the distortion is considered more important than the noise reduction of the signal.

Table 1 and 4 are related to the right arm for HT and ST, respectively; Table 2 and 5 are related to the shoulders and the facial sEMG for HT and ST, respectively; finally, the Table 3 and 6 represent the summary for the left arm with HT and ST, respectively. The LMU is present only for the soft thresholding (D. L Donoho 1995).

The first column indicates the algorithm. In each table the gray cell indicates the maximum value for the selected muscle, thresholding modification and α_{NR}.

Table 1 $DQ_{\%}$ Hard Thresholding – Right Arm

Algorithm	$DQ_{\%}$ R-ECU	$DQ_{\%}$ R-FCR	$DQ_{\%}$ R-BB	$DQ_{\%}$ R-TB	α_{NR}
BADA	90.3 ± 2.9	82.6 ± 3.4	82.6 ± 3.9	80.7 ± 1.9	0.7
UT	76.5 ± 2.2	68.0 ± 2.5	68.0 ± 2.0	73.0 ± 2.7	
SURE	85.6 ± 4.2	74.6 ± 1.3	74.6 ± 3.3	75.4 ± 0.8	
SMU	74.2 ± 3.5	68.8 ± 2.1	68.8 ± 1.6	50.1 ± 5.5	
SLMU	36.8 ± 0.4	45.0 ± 0.4	45.0 ± 0.4	42.0 ± 0.7	
LSMU	75.9 ± 3.7	70.1 ± 2.9	70.1 ± 1.6	51.7 ± 6.5	
GSMU	47.5 ± 1.4	60.1 ± 0.7	60.1 ± 0.6	44.0 ± 4.1	
BADA	94.5 ± 3.8	89.8 ± 8.0	93.7 ± 9.2	88.9 ± 4.5	0.3
UT	69.5 ± 5.2	65.4 ± 5.8	69.6 ± 4.6	82.8 ± 6.3	
SURE	91.7 ± 5.8	87.9 ± 3.0	90.4 ± 7.7	88.7 ± 2.0	
SMU	86.8 ± 8.2	83.6 ± 5.0	93.4 ± 3.7	68.8 ± 12.9	
SLMU	72.6 ± 1.0	76.0 ± 0.9	74.4 ± 0.9	74.2 ± 1.6	
LSMU	87.6 ± 8.5	82.3 ± 6.7	91.4 ± 3.8	65.5 ± 15.1	
GSMU	76.9 ± 3.3	82.4 ± 1.5	79.9 ± 1.3	71.5 ± 9.7	

Table 2 $DQ_{\%}$ Hard Thresholding – Shoulders and Face

Algorithm	$DQ_{\%}$ RT	$DQ_{\%}$ LT	$DQ_{\%}$ CS	$DQ_{\%}$ ZM	α_{NR}
BADA	73.2 ± 2.6	77.3 ± 2.9	69.8 ± 4.5	79.4 ± 6.8	0.7
UT	57.2 ± 1.2	58.0 ± 1.1	63.2 ± 4.0	66.8 ± 9.0	
SURE	50.7 ± 0.9	64.6 ± 1.4	56.0 ± 3.7	62.7 ± 8.0	
SMU	52.8 ± 4.3	59.0 ± 2.4	59.6 ± 4.3	67.0 ± 9.4	
SLMU	34.0 ± 0.4	37.4 ± 0.3	42.8 ± 0.5	41.0 ± 0.7	
LSMU	50.7 ± 4.0	52.2 ± 1.9	69.7 ± 4.5	69.7 ± 10.0	
GSMU	33.2 ± 3.5	38.4 ± 0.3	53.0 ± 3.5	40.6 ± 8.0	
BADA	83.4 ± 6.2	88.9 ± 6.8	71.1 ± 10.4	84.3 ± 15.8	0.3
UT	59.3 ± 2.9	56.7 ± 2.5	61.6 ± 9.4	68.1 ± 20.9	
SURE	77.3 ± 2.2	83.3 ± 3.3	65.0 ± 8.6	74.1 ± 18.6	
SMU	71.3 ± 10.0	80.7 ± 5.7	67.1 ± 10.0	60.5 ± 21.8	
SLMU	71.3 ± 0.9	73.0 ± 0.7	74.1 ± 1.2	73.5 ± 1.6	
LSMU	71.3 ± 9.3	77.9 ± 4.3	68.7 ± 10.4	63.9 ± 23.3	
GSMU	69.1 ± 8.1	73.4 ± 0.8	70.8 ± 8.1	62.0 ± 18.7	

Table 3 $DQ_{\%}$ Hard Thresholding – Left Arm

Algorithm	$DQ_{\%}$ L-ECU	$DQ_{\%}$ L-FCR	$DQ_{\%}$ L-BB	$DQ_{\%}$ L-TB	α_{NR}
BADA	85.4 ± 4.2	86.1 ± 4.0	91.9 ± 3.8	77.4 ± 3.7	0.7
UT	79.2 ± 3.5	76.1 ± 2.8	82.3 ± 3.0	70.6 ± 2.9	
SURE	76.8 ± 3.4	68.5 ± 1.8	86.5 ± 3.6	71.8 ± 3.2	
SMU	53.2 ± 3.8	49.3 ± 1.9	91.8 ± 1.5	76.8 ± 3.4	
SLMU	39.6 ± 0.8	39.6 ± 0.4	41.5 ± 0.3	51.5 ± 0.8	
LSMU	59.7 ± 4.2	56.2 ± 2.4	91.8 ± 1.4	77.4 ± 3.1	
GSMU	47.0 ± 1.6	39.1 ± 0.6	58.9 ± 0.4	68.8 ± 1.8	
BADA	91.9 ± 9.9	91.4 ± 9.2	92.3 ± 8.9	79.4 ± 8.7	0.3
UT	86.4 ± 8.2	74.9 ± 6.6	82.0 ± 7.0	67.9 ± 6.9	
SURE	88.6 ± 8.0	85.4 ± 4.1	92.1 ± 8.5	83.5 ± 7.4	
SMU	78.2 ± 8.8	75.7 ± 4.4	94.1 ± 3.4	76.5 ± 8.0	
SLMU	73.7 ± 1.8	73.8 ± 0.9	74.6 ± 0.6	78.4 ± 1.8	
LSMU	80.7 ± 9.8	77.3 ± 5.7	93.7 ± 3.2	77.5 ± 7.2	
GSMU	76.6 ± 3.8	73.5 ± 1.3	82.1 ± 0.9	83.1 ± 4.1	

Table 4 $DQ_{\%}$ Soft Thresholding – Right Arm

Algorithm	$DQ_{\%}$ R-ECU	$DQ_{\%}$ R-FCR	$DQ_{\%}$R-BB	$DQ_{\%}$R-TB	α_{NR}
BADA	87.6 ± 3.8	77.6 ± 2.5	84.3 ± 3.1	75.4 ± 1.6	0.7
UT	68.1 ± 0.7	62.1 ± 1.4	67.5 ± 0.7	65.5 ± 2.4	
SURE	80.5 ± 3.1	68.7 ± 1.9	77.0 ± 2.5	71.8 ± 1.7	
SMU	71.2 ± 4.0	64.1 ± 3.3	84.2 ± 2.3	44.7 ± 5.4	
LMU	32.8 ± 0.2	35.1 ± 0.1	34.1 ± 0.1	34.5 ± 0.2	
SLMU	72.2 ± 4.1	65.1 ± 3.8	79.7 ± 2.0	45.6 ± 5.4	
LSMU	45.8 ± 3.3	57.3 ± 2.1	51.9 ± 1.4	39.5 ± 5.2	
GSMU	20.1 ± 1.0	30.0 ± 1.6	26.0 ± 0.8	34.1 ± 2.2	
BADA	88.2 ± 8.8	77.9 ± 5.9	83.6 ± 7.2	80.5 ± 3.8	0.3
UT	49.8 ± 1.6	51.7 ± 3.3	54.0 ± 1.6	65.3 ± 5.7	
SURE	79.8 ± 7.2	74.0 ± 4.4	78.2 ± 5.9	80.1 ± 4.0	
SMU	71.1 ± 0.5	72.1 ± 0.3	71.7 ± 0.3	71.6 ± 0.5	
LMU	33.7 ± 2.2	41.1 ± 3.8	39.6 ± 1.9	55.7 ± 5.2	
SLMU	78.9 ± 9.6	70.7 ± 8.8	81.1 ± 4.6	51.3 ± 12.6	
LSMU	72.9 ± 7.8	76.0 ± 4.8	75.5 ± 3.2	61.2 ± 12.0	
GSMU	80.0 ± 9.3	72.5 ± 7.7	83.8 ± 5.3	56.3 ± 12.6	

Table 5 $DQ_{\%}$ Soft Thresholding – Shoulders and Face

Algorithm	$DQ_{\%}$ RT	$DQ_{\%}$ LT	$DQ_{\%}$ CS	$DQ_{\%}$ ZM	α_{NR}
BADA	66.9 ± 1.6	75.0 ± 2.5	67.5 ± 3.6	78.6 ± 6.9	0.7
UT	54.3 ± 0.8	54.4 ± 1.3	62.4 ± 2.9	64.7 ± 9.4	
SURE	44.3 ± 1.1	58.1 ± 1.2	52.7 ± 3.7	60.9 ± 7.7	
SMU	47.6 ± 4.1	55.9 ± 3.8	56.4 ± 3.7	63.8 ± 8.4	
LMU	31.8 ± 0.2	32.6 ± 0.1	35.5 ± 0.2	33.8 ± 0.3	
SLMU	45.6 ± 4.1	49.2 ± 3.5	67.4 ± 3.6	65.8 ± 8.5	
LSMU	29.8 ± 3.5	37.0 ± 1.9	48.9 ± 3.9	35.3 ± 8.7	
GSMU	20.5 ± 0.8	21.7 ± 1.1	31.1 ± 3.2	30.8 ± 9.1	
BADA	68.8 ± 3.8	83.5 ± 5.8	69.6 ± 8.5	82.4 ± 16.2	0.3
UT	52.5 ± 1.8	48.3 ± 3.0	59.8 ± 6.8	63.2 ± 22.0	
SURE	62.4 ± 2.5	68.2 ± 2.8	57.3 ± 8.7	69.9 ± 17.9	
SMU	70.6 ± 0.4	71.1 ± 0.2	72.0 ± 0.4	71.2 ± 0.6	
LMU	39.6 ± 1.8	36.2 ± 2.5	46.8 ± 7.5	49.9 ± 21.2	
SLMU	59.7 ± 9.5	70.8 ± 8.2	63.4 ± 8.5	54.9 ± 19.9	
LSMU	61.1 ± 8.2	69.9 ± 4.4	61.4 ± 9.1	49.6 ± 20.4	
GSMU	59.0 ± 9.6	73.4 ± 8.8	59.6 ± 8.7	53.0 ± 19.6	

Table 6 $DQ_{\%}$ Soft Thresholding – Left Arm

Algorithm	$DQ_{\%}$ L-ECU	$DQ_{\%}$ L-FCR	$DQ_{\%}$ L-BB	$DQ_{\%}$ L-TB	α_{NR}
BADA	84.0 ± 3.9	81.5 ± 3.1	89.2 ± 2.7	73.5 ± 2.7	0.7
UT	70.5 ± 2.1	68.0 ± 1.6	74.3 ± 1.5	67.6 ± 1.6	
SURE	75.1 ± 3.4	63.9 ± 2.6	83.0 ± 3.0	65.7 ± 2.5	
SMU	51.8 ± 3.9	44.6 ± 2.7	87.6 ± 1.7	72.6 ± 3.1	
LMU	33.6 ± 0.2	33.3 ± 0.1	34.5 ± 0.1	37.9 ± 0.2	
SLMU	57.8 ± 3.9	50.7 ± 3.2	86.4 ± 2.1	72.7 ± 2.8	
LSMU	45.9 ± 3.5	36.4 ± 1.8	56.5 ± 1.1	64.2 ± 2.7	
GSMU	30.9 ± 2.4	26.0 ± 1.8	30.2 ± 1.8	39.7 ± 1.9	
BADA	88.7 ± 9.1	80.8 ± 7.2	80.7 ± 6.3	76.0 ± 6.2	0.3
UT	66.2 ± 4.9	56.0 ± 3.7	63.4 ± 3.4	60.9 ± 3.8	
SURE	84.5 ± 8.0	74.8 ± 6.1	83.9 ± 7.0	69.3 ± 5.9	
SMU	71.4 ± 0.6	71.3 ± 0.3	71.9 ± 0.2	73.1 ± 0.5	
LMU	53.6 ± 5.5	42.1 ± 4.2	48.5 ± 4.1	50.7 ± 4.4	
SLMU	76.3 ± 9.0	64.4 ± 7.5	81.2 ± 4.9	66.5 ± 6.5	
LSMU	74.2 ± 8.2	67.3 ± 4.1	76.6 ± 2.5	72.4 ± 6.2	
GSMU	74.8 ± 9.2	64.8 ± 6.3	83.9 ± 4.0	66.7 ± 7.3	

The results show that the proposed BADA performs better in term of $DQ_{\%}$ both in case of α_{NR}=0.7 and α_{NR}=0.3 for almost all the muscles under observation. In particular, when the algorithm did not perform as the best, the value is very near to the maximum one. In case of the forearm muscles (R-ECU, R-FCR, L-ECU and L-FCR), that are the one more stressed for

this kind of exercise, the BADA algorithm always performs better than the others and only the SURE can be considered comparable (Table 1 and 4, second and third columns).

The muscles, for which the BADA underperforms, are the CS, L-BB and R-BB. These muscles are used very few times with low activation during the peg-board exercise and the noise component is the main factor; in this case the ER component is negligible. Based on this consideration we tried the case of α_{NR}=1 and α_{ER}=0 for R-BB, L-BB and CS (Table 7): the BADA clearly outperforms the other algorithms, especially for the L-BB and R-BB. The table shows the thresholding modification (HT or ST) on the last column.

Table 7 Hard and Soft Thresholding with α_{NR}=1 and α_{ER}=0

Algorithm	$DQ_{\%}$ R-BB	$DQ_{\%}$ L-BB	$DQ_{\%}$ CS	*Thresholding*
BADA	74.6 ± 0.0	75.8 ± 0.0	76.4 ± 0.0	HT
UT	65.7 ± 0.0	65.8 ± 0.0	71.7 ± 0.0	
SURE	65.5 ± 0.0	54.1 ± 0.0	65.3 ± 0.0	
SMU	56.7 ± 0.0	55.8 ± 0.0	74.4 ± 0.0	
SLMU	36.0 ± 0.0	71.9 ± 0.0	51.4 ± 0.0	
LSMU	17.9 ± 0.0	16.6 ± 0.0	71.4 ± 0.0	
GSMU	41.4 ± 0.0	74.1 ± 0.0	58.5 ± 0.0	
BADA	75.6 ± 0.0	74.8 ± 0.0	77.5 ± 0.0	ST
UT	66.6 ± 0.0	67.3 ± 0.0	72.7 ± 0.0	
SURE	63.7 ± 0.0	42.3 ± 0.0	63.1 ± 0.0	
SMU	56.7 ± 0.0	48.1 ± 0.0	61.4 ± 0.0	
LMU	66.0 ± 0.0	54.0 ± 0.0	77.1 ± 0.0	
SLMU	47.9 ± 0.0	59.8 ± 0.0	31.4 ± 0.0	
LSMU	46.4 ± 0.0	70.4 ± 0.0	77.4 ± 0.0	
GSMU	53.3 ± 0.0	39.6 ± 0.0	58.1 ± 0.0	

Additionally, the BADA shows consistency in term of values with the different values of α_{NR}, HT and ST. In Figure 7 the R-ECU averaged results for the cases of α_{NR}=0.3 and α_{ER}=0.7, α_{NR}=0.7 and α_{ER}=0.3 for both HT and ST are plotted.

Figure 8 shows a portion of the original sEMG signal (R-ECU) during one activation, together with the differences with the signals denoised by UT HT, BADA HT, SURE HT, SLMU HT and GSMU HT. It is evident that while the UT HT (c) denoises the baseline, it also considerably distorts the signal. The SLMU HT and GSMU HT cannot eliminate completely the baseline, in fact the difference in the first portion of the signal is very small. The SLMU HT, in particular, is very similar to the

original signal. The SURE HT and BADA show similar visual performance: the baseline is well denoised while the shape of the signal during the activation is not distorted. The BADA, however, is more stable than the SURE, especially in the transition between the Baseline and the exercise, where the SURE distorts the signal.

Figure 7 Comparison of the algorithms for the R-ECU.

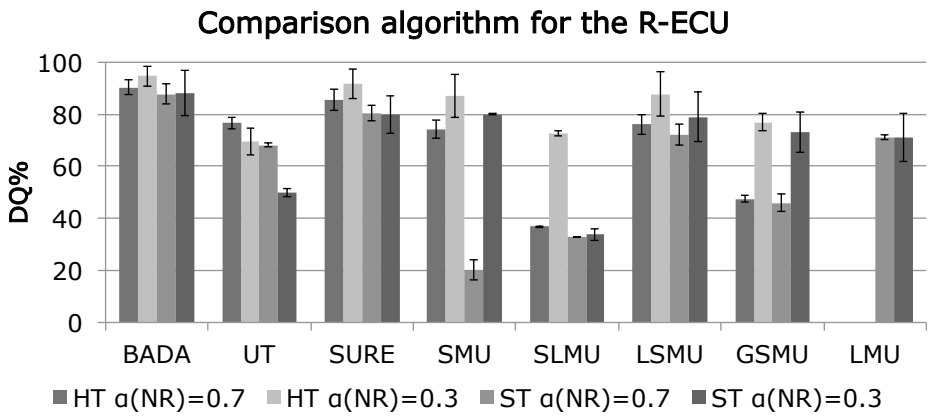

Figure 8 Original signal (a); difference between the original signal and the signal denoised by BADA HT (b), UT HT (c), SURE HT (d), SLMU HT (e) and GSMU HT (f). The last chart indicate the time axis.

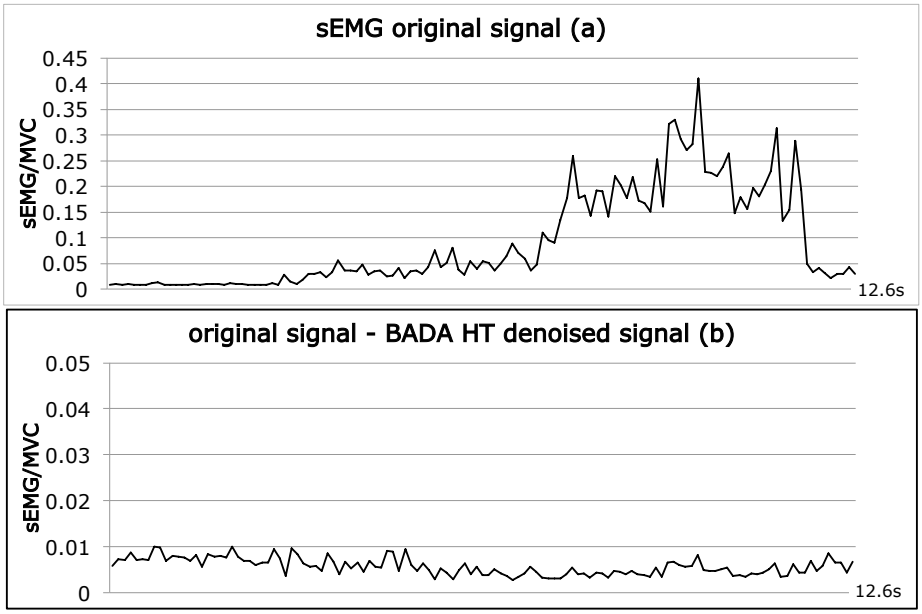

Author

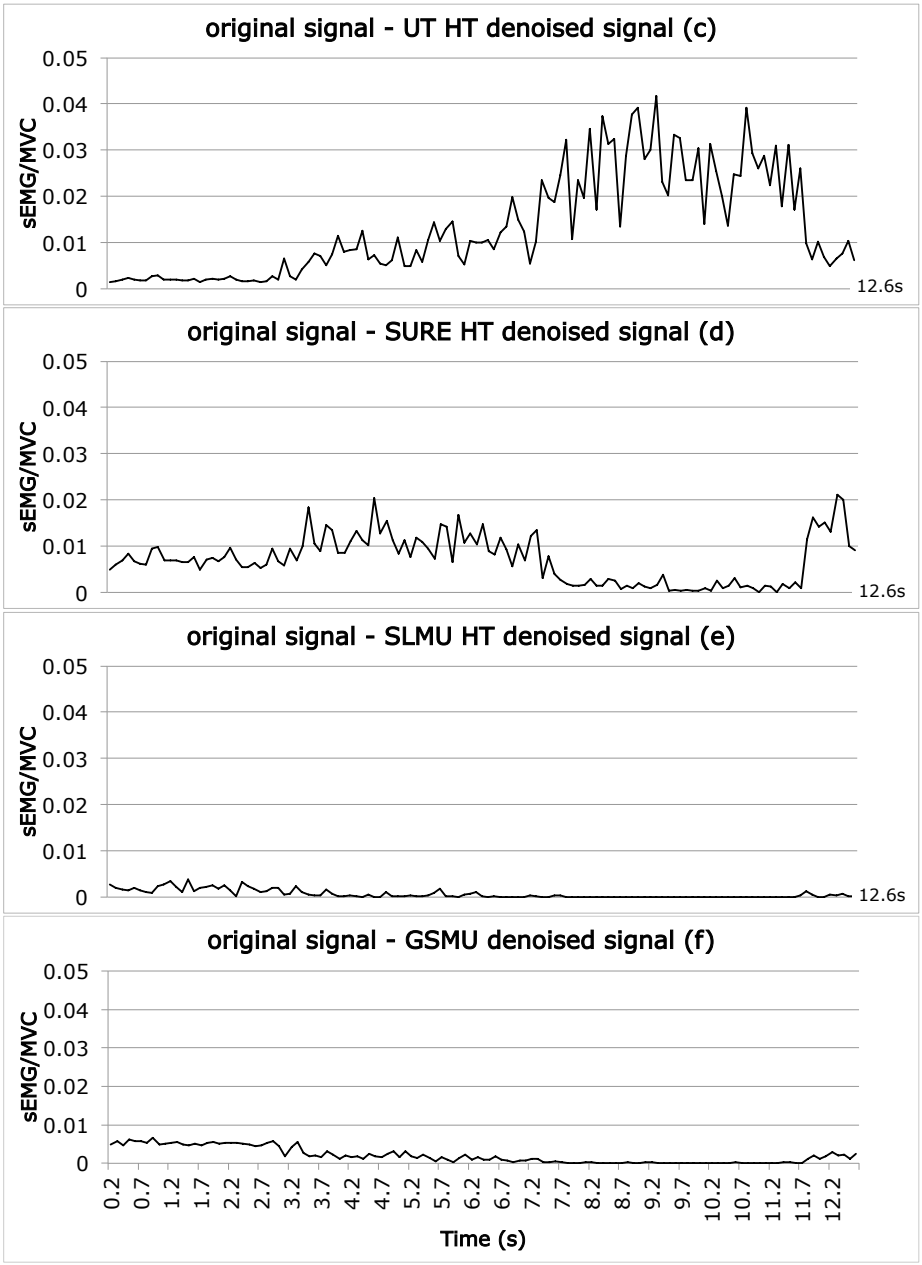

Conclusions

In this paper we have introduced a new technique to denoise a sEMG signal by using its baseline to estimate the thresholds to apply to the wavelet thresholding algorithm. The proposed adaptive technique, namely Baseline Adaptive Denoising Algorithm (BADA), has shown better

performances than standard Donoho method (universal threshold) and different its variations, in term of noise cancellation and signal distortion, quantified by a new proposed indicator of denoising quality, considering the linear weighted combination of Noise Ratio and Normalized Signal Distortion. Among the variations of the Donoho method, we have noticed that the SURE-based thresholding estimation was the one that showed similar coherence to the proposed technique for hard and soft thresholding. We have extensively used our algorithm for the denoising of sEMG signal in various experiments, in particular for the biomechanical analysis of the arms and forearms in the training of young surgeons. The final goal is the detection of activations of the muscles of arms, their connection with the movements of the hands, together with the shoulders muscles (mainly the trapezius) to estimate the fatigue during the various training. We suggest readers to try the proposed algorithm for the denoising of images: in that case the baseline could be considered as portion of image with noise, previously identified.

Acknowlegments

This research has been supported by the G-COE Global Robot Academia Program in Waseda University, Japan and partially by a Grant by STMicroelectronics. This research has been conducted at Humanoid Robotics Institute, in collaboration with the G-COE Global Robot Academia. The authors would like to express their gratitude to Okino Industries LTD, Japan ROBOTECH LTD, SolidWorks Corp, Dyden, for their support to the research. Eventually, the authors would like to thank the 15 volunteers who kindly accepted to take part in the experiment.

References

Bartolomeo, L. et al., 2011. Baseline Adaptive Wavelet Thresholding Technique for sEMG Denoising T. D. Pham et al., eds. *AIP Conference Proceedings*, 1371(1), pp.205-214.

Basmajian, J.V. and Luca, C.D., 1985. *Muscles Alive: Their Functions Revealed by Electromyography* 5th ed., Lippincott Williams and Wilkins.

Blancovelasco, M., Weng, B. and Barner, K., 2008. ECG signal denoising and baseline wander correction based on the empirical mode decomposition. *Computers in Biology and Medicine*, 38(1), pp.1-13.

Ching-Fen Jiang and Shou-Long Kuo, 2007. A Comparative Study of Wavelet Denoising of Surface Electromyographic Signals. In *Engineering in Medicine and Biology Society, 2007. EMBS 2007. 29th Annual International Conference of the IEEE*.

Coifman, R. and Donoho, DL, 1995. Translation invariant de-noising. *Wavelets and Statistics*, Springer Lecture Notes in Statistics 103. New York: Springer-Verlag, 1994, pp. 125–150.

Cram, J.R., Ph.D., Kasman, G.S. and Holtz, J., 1998. *Introduction to Surface Electromyography* 1st ed., Jones and Bartlett Publishers.

Derossis, A.M. et al., 1998. Development of a Model for Training and Evaluation of Laparoscopic Skills. *The American Journal of Surgery*, 175(6), pp.482-487.

Donoho, David and Johnstone, I.M., 1994. Ideal spatial adaptation by wavelet shrinkage. *Biometrika*, 81(3), pp.425 -455.

Donoho, David, 1995. De-noising by soft-thresholding. *IEEE Transactions on Information Theory*, 41(3), pp.613-627.

Donoho, David and Johnstone, I.M., 1995. Adapting to Unknown Smoothness via Wavelet Shrinkage. *Journal of the American Statistical Association*, 90, p.1200--1224.

Donoho, David , 1993. Wavelet Shrinkage and W.V.D.: A 10-minute tour. *Progress in Wavelet analysis and applications*, p.109-128.

Gazzoni, M., 2010. Multichannel surface electromyography in ergonomics: Potentialities and limits. *Human Factors and Ergonomics in Manufacturing and Service Industries*, 20(4), pp.255-271.

Guoxiang, S. and Ruizhen, Z., 2001. Three Novel Models of Threshold Estimator for Wavelet Coefficients. In Y. Y. Tang et al., eds. *Wavelet Analysis and Its Applications*. Berlin, Heidelberg: Springer Berlin Heidelberg, pp. 145-150.

Hernandez, C. et al., 2010. Traditional sEMG fatigue indicators applied to a real-world sport functional activity: Roundhouse kick. In *Electronics, Communications and Computer (CONIELECOMP), 2010 20th International Conference on*. Electronics.

Huigen, E., Peper, A. and Grimbergen, C.A., 2002. Investigation into the origin of the noise of surface electrodes. *Medical and Biological Engineering and Computing*, 40(3), pp.332-338.

Johnstone, I.M. and Silverman, B.W., 1997. Wavelet Threshold Estimators for Data with Correlated Noise. *Journal of the Royal Statistical Society. Series B (Methodological)*, 59(2), pp.319-351.

Kibler, W.B. et al., 2008. Electromyographic Analysis of Specific Exercises for Scapular Control in Early Phases of Shoulder

Rehabilitation. *The American Journal of Sports Medicine*, 36(9), pp.1789 -1798.

Knudson, D. and Blackwell, J., 2000. Trunk muscle activation in open stance and square stance tennis forehands. *International Journal of Sports Medicine*, 21(5), pp.321-324.

Lange, G.W. et al., 1996. Electromyographic and kinematic analysis of graded treadmill walking and the implications for knee rehabilitation. *The Journal of Orthopaedic and Sports Physical Therapy*, 23(5), pp.294-301.

Lin, Zhuohua and al, 2010. Objective Evaluation of Laparoscopic Surgical Skills Using Waseda Bioinstrumentation System WB-3. In *IEEE International Conference on Robotics and Biomimetics (Robio 2010)*.

De Luca, C.J., 1997. The Use of Surface Electromyography in Biomechanics. *Journal of Applied Biomechanics*. Vol 13, p 135-163; 1997

De Luca, C.J. et al., 2010. Filtering the surface EMG signal: Movement artifact and baseline noise contamination. *Journal of Biomechanics*, 43(8), pp.1573-1579.

Merletti, Roberto and Parker, P., 2004. *Electromyography: Physiology, Engineering, and Non-Invasive Applications* 1st ed., Wiley-IEEE Press.

Phinyomark, Angkoon, Limsakul, Chusak and Phukpattaranont, Pornchai, 2009. A Comparative Study of Wavelet Denoising for Multifunction Myoelectric Control. In *Proceedings of the 2009 International Conference on Computer and Automation Engineering*.

Phinyomark, A., Limsakul, C. and Phukpattaranont, P., 2009. EMG denoising estimation based on adaptive wavelet thresholding for multifunction myoelectric control. In *Innovative Technologies in Intelligent Systems and Industrial Applications, 2009. CITISIA 2009*.

Rosas-Orea et al., 2005. A Comparative Simulation Study of Wavelet Based Denoising Algorithms. In *15th International Conference on Electronics, Communications and Computers (CONIELECOMP'05)*.

Shensa, M.J., 1992. The discrete wavelet transform: wedding the a trous and Mallatalgorithms. *IEEE Transactions on Signal Processing*, 40(10), pp.2464-2482.

Shi Zhong and Cherkassky, V., 2000. Image denoising using wavelet thresholding and model selection. In *2000 International*

Conference on Image Processing, 2000. Proceedings. pp. 262-265 vol.3.

Stein, C.M., 1981. Estimation of the Mean of a Multivariate Normal Distribution. *The Annals of Statistics*, 9(6), pp.1135-1151.

Troiano, A. et al., 2008. Assessment of force and fatigue in isometric contractions of the upper trapezius muscle by surface EMG signal and perceived exertion scale. *Gait and Posture*, 28(2), pp.179-186.

Zecca, M. et al., 2002. Control of Multifunctional Prosthetic Hands by Processing the Electromyographic Signal. *Critical Reviews in Biomedical Engineering*, 30(4-6), pp.459-485.